

Cite this: *CrystEngComm*, 2012, 14, 7275–7286

www.rsc.org/crystengcomm

PAPER

The supramolecular assemblies of 7-amino-2,4-dimethylquinolinium salts and the effect of a variety of anions on their luminescent properties†

Qing Su, Mina He, Qiaolin Wu,* Wei Gao, Hai Xu, Ling Ye and Ying Mu*

Received 13th February 2012, Accepted 20th July 2012

DOI: 10.1039/c2ce25883h

The 7-amino-2,4-dimethylquinolinium salts with a variety of anions (Cl^- , HCOO^- , CH_3COO^- , PhCOO^- , $\text{L-HOOCCH(OH)CH(OH)COO}^-$) have been synthesized and characterized. The crystal structures of these salts were determined by single-crystal X-ray diffraction. The structure analysis confirms that the nitrogen atoms in the quinoline rings are protonated in all salts. The two solvates have been obtained and thereby provide a useful complement to cocrystal screening. All the quinolinium salts display interesting three dimensional supramolecular networks. The hydrogen bonding interactions observed in all of the salts are $\text{N-H}\cdots\text{O}$, $\text{O-H}\cdots\text{O}$ and $\text{N-H}\cdots\text{Cl}$, together with weak $\text{C-H}\cdots\text{O}$, $\text{C-H}\cdots\text{N}$, $\text{C-H}\cdots\text{Cl}$ hydrogen bonds. The weak $\text{C/N-H}\cdots\pi$ contacts and π - π stacking interactions involving the quinoline moieties also exist in quinolinium salts. The observed noncovalent interactions become prominent in stabilizing their crystal packing. The 7-amino-2,4-dimethylquinolinium salts show strong luminescence in the solid state and solution in the range 422–534 nm. The solid-state emission spectra of the quinolinium salts are sensitive to the anion species, and highly dependent on the nature of the stacking interactions.

Introduction

Noncovalent interactions such as hydrogen bonding, ionic interactions, metal coordination, and π - π interactions, as well as other weak forces play crucial roles in many fields, such as supramolecular chemistry, host-guest chemistry, biochemistry, pharmaceutical chemistry, molecular recognition, and materials science.^{1–3} In recent years, many efforts have been focused on investigating these interactions and clarifying their relationship to supramolecular structures.⁴ As an example of one of the most sophisticated supramolecular systems, the double-helical DNA structure⁵ is assembled through multiple Watson-Crick hydrogen bonding and π - π stacking interactions, offering significant opportunities to mimic nature's systems for fundamental studies and numerous biochemical and biomedical applications.⁶ In the case of active pharmaceutical ingredients (APIs), the different solid forms such as solvates, hydrates, polymorphs, salts and cocrystals with tailoring biopharmaceutical properties have been explored systematically,⁷ which are relevant with supramolecular synthesis and crystal engineering. Most of these investigations indicate that the combination of hydrogen bonding and/or other weak interactions has been used as a very powerful and versatile

strategy in the formation of supramolecular assemblies. Recently, the various hydrogen bonding patterns involving pyridine-carboxylate interactions are of significance in crystal engineering.⁸ Moreover, the $\text{N-H}\cdots\text{O/N}$ and $\text{O-H}\cdots\text{O}$ hydrogen bonds, together with weak $\text{C-H}\cdots\text{O/N}$ hydrogen bonds have been used in the design of a number of supramolecular nanoarchitectures, layers, rosettes, rods, tubes, tapes, ribbons, sheets, and spheres aggregates.⁹ In addition, It is well known that the hydrogen bonding interactions between carboxylate groups and the pyrimidine moieties have been considered as the models for protein-nucleic acid recognition and drug-receptor recognition. Supramolecular architectures based on molecular recognition between complementary molecular components and self-assemblies of organic molecules with the assistance of non-covalent forces are of current interest.¹⁰

We have previously reported a series of Schiff zinc(II) complexes containing 7-amino-2,4-dimethylquinolinyl with a variety of coordination geometries by modifications of the ligand denticity, the ligand-to-metal ratio, and non-covalent interactions.¹¹ In our previous studies, an organic salt of 7-amino-2,4-dimethylquinoline with formic acid has also been reported,¹² and the result reveals that the nitrogen atom in the pyridine ring is protonated when the carboxyl is deprotonated, and the crystal packing is stabilized by $\text{N-H}\cdots\text{O}$ hydrogen bonds and π - π stacking interactions. The adjacent chains are held together by $\text{N-H}\cdots\text{O}$ hydrogen bonds with a rectangular cavity. Very recently, we have focused our continuing efforts on the construction of well-defined supramolecular structures of 7-amino-2,4-dimethylquinolinium salts, and understanding the

State Key Laboratory for Supramolecular Structure and Materials, School of Chemistry, Jilin University, 2699 Qianjin Street, Changchun, 130012, People's Republic of China. E-mail: wuql@jlu.edu.cn; ymu@jlu.edu.cn; Fax: (+86)-431-5193421; Tel: (+86)-431-5168376

† Electronic Supplementary Information (ESI) available: CCDC reference numbers 294744, 866261–866264. Crystallographic data in CIF or other electronic format. Synthetic route of the quinolinium salts in Schemes S1 and S2. The photophysical data in Table ST-1. See DOI: 10.1039/c2ce25883h

anion effects on the supramolecular assemblies and luminescent properties of 7-amino-2,4-dimethylquinolinium salts. The hydrogen chloride, formic acid, acetic acid, benzoic acid, and L-tartaric acid were chosen for this study mainly because those Lewis acids with different volumes of the anion are good for selective and directional geometry-based crystal design to generate interesting supramolecular architectures. Notably, the crystal packing should be dominated by strong hydrogen bonding N–H⋯O and much weaker C–H⋯N, C–H⋯π and π–π interactions. Herein, we wish to report the supramolecular assemblies of a series of 7-amino-2,4-dimethylquinolinium salts, as well as the anion effects on both crystal packing and their luminescent properties in the solid state and solution.

Experimental

Materials and general comments

Starting materials and solvents such as *m*-phenylenediamine, acetylacetone, triethylamine, acetic acid, formic acid, concentrated hydrogen chloride, benzoic acid, L-tartaric acid, methylene chloride, dimethyl sulphone (DMSO) and ethanol (95%) were commercially obtained and used as received. The elemental analyses were performed on a Perkin-Elmer 2400 analyzer. ¹H NMR spectra were recorded on a Varian Mercury 300 MHz or a Bruker ACF 500 MHz spectrometer. IR spectra were recorded on a Nicolet Impact 410 FTIR spectrometer using KBr pellets. UV-vis spectra were obtained on a Perkin-Elmer Lambda 20 spectrometer. Luminescence spectra were measured on a Perkin-Elmer LS55 Luminescence spectrometer at room temperature.

7-Amino-2,4-dimethylquinolinium chloride (1·HCl)

To a solution of *m*-phenylenediamine (5.30 g, 49.0 mmol) in 30 mL of ethanol was added a mixture of concentrated HCl (4.0 mL, 49.0 mmol) and acetylacetone (5.0 mL, 49.0 mmol) in 30 mL of ethanol at room temperature. The mixture was stirred until a large amount of yellow solid precipitated. The solid was collected by filtration, washed with ethanol and dried. Yield: 7.98 g, 78.0%. Anal. Calcd for C₁₁H₁₃N₂Cl (208.69): C, 63.31; H, 6.28, N, 13.42. Found: C, 63.37; H, 6.25; N, 13.49. ¹H NMR (D₂O, 300 MHz, 298 K): δ 2.34 (s, 3H, CH₃), 2.41(s, 3H, CH₃), 2.57 (m, DMSO in crystal), 6.10 (s, 1H, 8-*H*), 6.69 (d, 1H, 6-*H*), 6.81 (s, 1H, 3-*H*), 7.37 (d, 1H, 5-*H*) ppm. IR (KBr, cm⁻¹): 3371 (m), 3306 (m), 3202 (s), 2908 (m), 2848 (m), 2739 (m), 1931 (w), 1842 (w), 1770 (w), 1641 (vs), 1594 (s), 1475 (m), 1448 (m), 1387 (m), 1245 (w), 1290 (w), 1199 (m), 1155 (w), 1056 (w), 1033 (m), 930 (m), 848 (m), 791 (w), 721 (w), 664 (w), 593 (w), 542 (w).

7-Amino-2,4-dimethylquinoline (1)

To a solution of 1·HCl (3.13 g, 15.0 mmol) in 40 mL of water was added a mixture of 40 mL of CH₂Cl₂ and 3.0 mL of NEt₃. The mixture was stirred at room temperature for 2 h. The organic layer was separated and the aqueous layer was further extracted with CH₂Cl₂ (3 × 10 mL). The combined organic layers were dried over anhydrous MgSO₄, filtered, and concentrated *in vacuo*. The yellowish solid was collected by filtration, washed with ethyl ether and dried. Yield: 1.70 g, 66%. Anal. Calcd for C₁₁H₁₂N₂ (172.23): C, 76.71; H, 7.02, N, 16.27. Found: C, 76.68; H, 7.07; N, 16.21. ¹H NMR (CDCl₃, 500 MHz,

298 K): δ 2.58 (s, 3H, CH₃), 2.63 (s, 3H, CH₃), 4.02 (s, 2H, NH₂), 6.89 (s, 1H, 3-*H*), 6.93 (d, 1H, 6-*H*), 7.18 (s, 1H, 8-*H*), 7.75 (d, 1H, 5-*H*) ppm. ¹³C NMR (CDCl₃, 125.75 MHz, 298 K): δ 18.4 (CH₃), 25.1 (CH₃), 109.5, 117.1, 119.6, 120.2, 124.7, 143.9, 147.5, 149.5, 158.8 ppm. IR (KBr, cm⁻¹): 3370 (s), 3307 (m), 3180 (s), 3026 (m), 2949 (m), 2920 (m), 2855 (m), 2745 (w), 1885 (w), 1640 (s), 1597 (s), 1525 (s), 1421 (s), 1356 (m), 1291 (m), 1236 (m), 1151 (m), 1126 (w), 1068 (w), 1027 (w), 884 (w), 844 (m), 815 (m), 772 (w), 707 (w), 662 (m), 599 (m), 543 (w).

7-Amino-2,4-dimethylquinolinium formate (1·HCOOH)

To a solution of 7-amino-2,4-dimethylquinoline (0.31 g, 1.80 mmol) in 10 mL of ethanol was added 0.07 mL of formic acid (1.80 mmol) at room temperature. After stirring for 0.5 h, the volatile materials were removed *in vacuo*. The residue was washed with ethyl ether and dried to give yellow-green solid. Yield: 0.37 g, 95%. Anal. Calcd for C₁₂H₁₄N₂O₂ (218.25): C 66.04, H 6.47, N 12.84; Found: C 66.15, H 6.51, N 12.78. ¹H NMR (D₂O, 300 MHz, 298 K): δ 2.37 (s, 3H, CH₃), 2.41 (s, 3H, CH₃), 6.26 (s, 1H), 6.76 (d, 1H), 6.84 (d, 1H), 7.46 (s, 1H), 8.24 (s, 1H, HCOO) ppm.

7-Amino-2,4-dimethylquinolinium acetate (1·CH₃COOH)

1·CH₃COOH was synthesized by the same conditions and procedures as for 1·HCOOH with acetic acid as a starting material. 1·CH₃COOH was obtained as yellow-green solid. Yield: 0.39 g, 94%. Anal. Calcd for C₁₃H₁₆N₂O₂ (232.28): C 67.22, H 6.94, N 12.06; Found: C 67.30, H 6.88, N 12.15. ¹H NMR (CDCl₃, 300 MHz, 298 K): δ 2.10 (s, 3H, CH₃COO), 2.60 (s, 3H, CH₃), 2.73 (s, 3H, CH₃), 6.89 (s, 1H), 6.93 (d, 1H), 7.41 (s, 1H), 7.73 (d, 1H) ppm.

7-Amino-2,4-dimethylquinolinium benzoate (1·PhCOOH)

1·PhCOOH was synthesized by the same conditions and procedures as for 1·HCOOH with benzoic acid as starting material. 1·PhCOOH was obtained as brown-yellow solid. Yield: 0.49 g, 93%. Anal. Calcd for C₁₈H₁₈N₂O₂ (294.35): C 73.45, H 6.16, N 9.52; Found: C 73.38, H 6.20, N 9.46. ¹H NMR (D₂O, 300 MHz, 298 K): δ 2.28 (s, 3H, CH₃), 2.36 (s, 3H, CH₃), 6.10 (s, 1H), 6.67 (d, *J* = 9.3 Hz, 1H), 6.72 (s, 1H), 7.18 (t, *J* = 6.9 Hz, 2H), 7.25 (d, *J* = 6.0 Hz, 1H), 7.32 (d, *J* = 9.0 Hz, 1H), 7.68 (d, *J* = 8.1 Hz, 2H) ppm.

7-Amino-2,4-dimethylquinolinium L-tartrate (1·L-tartaric acid)

To a solution of 7-amino-2,4-dimethylquinoline (0.31 g, 1.80 mmol) in 10.0 mL of ethanol was added a solution of L-tartaric acid (0.27 g, 1.80 mmol) in 8.0 mL of ethanol at room temperature. The mixture was stirred until a large amount of yellow solid precipitated. The solid was collected by filtration, washed with ethanol and dried. Pure 1·L-tartaric acid was obtained as yellow solid after recrystallization from ethanol. Yield: 0.53 g, 91%. Anal. Calcd for C₁₅H₂₈N₂O₆ (322.31): C 55.90, H 5.63, N 8.69; Found: C 55.95, H 5.60, N 8.62. ¹H NMR (D₂O, 300 MHz, 298 K): δ 2.41 (s, 3H, CH₃), 2.43 (s, 3H, CH₃), 4.36 (s, 2H, CHOH), 6.14 (s, 1H), 6.70 (d, *J* = 9.0 Hz, 1H), 6.81 (s, 1H), 7.40 (d, *J* = 9.3 Hz, 1H) ppm.

Single-crystal X-ray diffraction

The single crystal X-ray diffraction data for compounds **1·HCl**, **1·HCl·DMSO**, **1·HOAc**, **1·PhCOOH**, and **1·L-tartaric acid·2H₂O** were collected on a Rigaku R-AXIS RAPID IP diffractometer equipped with graphite-monochromated Mo-K α radiation ($\lambda = 0.71073$ Å), operating at 293 ± 2 K. The structures were solved by direct method¹³ and refined by full-matrix least squares based on F^2 using the SHELXTL 5.1 software package.¹⁴ All non-hydrogen atoms were refined anisotropically. Unless otherwise noted, hydrogen atoms were included in idealized position and were allowed to ride. The details of crystallographic collection and refinement data are given in Table 1. The hydrogen bonding parameters are given in Table 2 and Table 3.

Results and discussion

Synthesis and characterization

7-Amino-2,4-dimethylquinoline hydrochloride (**1·HCl**) was obtained by the reaction of *m*-phenylenediamine (MPD) with acetylacetone (acac) in the presence of conc. HCl at room temperature (see Scheme S1, ESI[†]). It has proved to be an efficient and simple method for the high-yielding and large-scale synthesis of **1·HCl**. The alcoholic filtrate could be distilled and recycled. The reaction for the preparation of **1·HCl** was also tested in DMF or methanol, but it was found that the yield is lower than the one in ethanol. The reaction was also examined with different molar ratios of acac/MPD/conc. HCl and **1·HCl** was always obtained when the molar ratio is 1 : 1 : 1, 2 : 1 : 1 or 1 : 2 : 1 in EtOH at room temperature. Compound **1** was feasibly synthesized in higher yield by treatment of **1·HCl** with triethylamine in methylene chloride/water, which is a new efficient method for the preparation of Compound **1**.¹⁵ **1·HCOOH**, **1·CH₃COOH**, **1·PhCOOH** and **1·L-tartaric acid** were obtained by the reaction of 7-amino-2,4-dimethylquinoline with the corresponding acid in similar yields at room temperature (see Scheme S2, ESI[†]). Compound **1** and **1·HCl**, **1·HCOOH**, **1·CH₃COOH**, **1·PhCOOH** and **1·L-tartaric acid** were characterized by elemental analysis and ¹H NMR.

Structures of quinolinium compounds **1·HCl**, **1·HCl·DMSO**, **1·CH₃COOH**, **1·PhCOOH**, **1·L-tartaric acid·2H₂O**

The crystals of compounds **1·HCl·DMSO**, **1·PhCOOH** and **1·L-tartaric acid·2H₂O** suitable for X-ray crystal structure determination were slowly grown from DMSO at room temperature. The crystals of **1·HCl** and **1·CH₃COOH** suitable for X-ray crystal structure determination were slowly grown from EtOH at room temperature. The structures of **1·HCl**, **1·HCl·DMSO**, **1·CH₃COOH**, **1·PhCOOH** and **1·L-tartaric acid** were determined by single crystal X-ray diffraction analysis. The ORTEP drawings of molecule structures are shown in Fig. 1.

7-Amino-2,4-dimethylquinolinium chloride crystallizes in the triclinic space group $P\bar{1}$. The asymmetric unit of **1·HCl** contains two independent molecules A and B, and molecule A is shown in Fig. 1. In the packing of **1·HCl** (Fig. 2), there are N1–H \cdots Cl hydrogen bonds and weak C–H \cdots Cl hydrogen bonds. The Cl1 and Cl2 atoms have different hydrogen bonding environments. There are seven hydrogen bonds around Cl1 atom, being C7–H7 \cdots Cl1, C10–H10C \cdots Cl1, C18–H18 \cdots Cl1, C21–H21C \cdots Cl1, N1–H100 \cdots Cl1,

N2–H102 \cdots Cl1 and N4–H104 \cdots Cl1, respectively. Meanwhile, there are only four hydrogen bonds around Cl2 atom, being C22–H22C \cdots Cl2, N2–H101 \cdots Cl2, N3–H103 \cdots Cl2, N4–H105 \cdots Cl2, respectively. The molecule A forms a 1-D infinite chain through N1–H100 \cdots Cl1 and N2–H102 \cdots Cl1 hydrogen bonds. There are also weak C7–H7 \cdots Cl1 interactions, which form a graph-set motif $R_2^1(6)$ together with N2–H102 \cdots Cl1 hydrogen bonds. The adjacent quinoline rings in the π -stacking interactions are antiparallel with the centroid–centroid distances of 3.35 to 3.49 Å (3.35/3.42 Å for the rings of molecule A; 3.46/3.49 Å for the rings of molecule B). The 1-D infinite chains were linked through C10–H10C \cdots Cl1 interactions and π – π interactions with the adjacent quinoline rings to form a 2-D layer structure (Fig. 2b). The molecule B forms a dimer through N3–H103 \cdots Cl2 and N4–H105 \cdots Cl2 hydrogen bonds with a graph-set motif $R_4^2(16)$. The dimers were connected through C22–H22C \cdots Cl2 and π – π interactions into a ladder structure (Fig. 2c). The 2-D layer structure and ladder structure were further linked through N4–H104 \cdots Cl1, C18–H18 \cdots Cl1, C21–H21C \cdots Cl1 and N2–H101 \cdots Cl2 interactions to form 3-D network (Fig. 2a).

In addition to **1·HCl**, the **1·HCl** solvates have been obtained in the cocrystallization experiments. Moreover, the structure of the 1 : 1 solvate has revealed the interesting changes in the hydrogen bonding patterns, resulting in the different three-dimensional network. In the asymmetric unit of **1·HCl·DMSO**, there is one **1·HCl** molecule and one solvent DMSO molecule. In the packing of the **1·HCl·DMSO** (Fig. 3), there are N2–H2B \cdots Cl1 and C8–H8 \cdots Cl1 interactions with the graph-set motif $R_2^1(6)$. The adjacent molecules were linked by the N1–H1 \cdots Cl1 hydrogen bonds to form 1-D S-shape chain (Fig. 3b). The adjacent chains formed the layer structure *via* the intermolecular π – π interaction between adjacent quinoline rings with the separation distance of 3.32 Å. The neighbouring DMSO molecules form cyclic $R_2^2(8)$ dimer through C–H \cdots O hydrogen bonds, and the dimers were further linked through C–H \cdots O hydrogen bonds to form 1-D S-shape chain (Fig. 3c). The layer structure and the 1-D S-shape chain formed by DMSO molecules were further linked into the final 3-D network through N2–H2A \cdots O1 hydrogen bonds.

The 1 : 1 organic salt of 7-amino-2,4-dimethylquinoline and formic acid has been reported by our group¹². A clearer packing diagram is shown in Fig. 4. In the packing of **1·HCOOH**, there exist not only strong N–H \cdots O hydrogen bonds but also weak C–H \cdots O interactions. The quinolinium cations and formate anions form chains through strong N–H \cdots O hydrogen bonds and C–H \cdots O interactions with the graph-set motifs $R_2^1(6)$ and $R_2^2(8)$. Two other N–H \cdots O hydrogen bonds link adjacent chains into a grid with a rectangular cavity and a graph-set motif $R_4^4(20)$ to form a 2-D sheet. The adjacent sheets were linked through C11–H11C \cdots O2, C11–H11B \cdots O1 and π – π interactions to form 3-D network.

7-Amino-2,4-dimethylquinolinium acetate crystallizes in the orthorhombic space group $Pbca$. The asymmetric unit contains one acetate and one 7-amino-2,4-dimethylquinolinium. In the crystal packing diagram (Fig. 5), two acetate and two 7-amino-2,4-dimethylquinolinium form a staircase-like dimer through four N–H \cdots O hydrogen bonds. The dimer was further stabilized by weak C–H \cdots O interactions. Meanwhile, the dimers were linked by other N–H \cdots O hydrogen bonds and C–H \cdots O interactions to form 3-D network. There also exist π – π interactions between the adjacent quinoline rings with the

Table 1 Crystal data and structure refinement for compounds 1·HCl, 1·HCl·DMSO, 1·CH₃COOH, 1·PhCOOH and 1·L-tartaric acid·2H₂O

Data	1·HCl	1·HCl·DMSO	1·CH ₃ COOH	1·PhCOOH	1·L-tartaric acid·2H ₂ O
Formula	C ₁₁ H ₁₃ ClN ₂	C ₁₃ H ₁₉ ClN ₂ O ₅	C ₁₃ H ₁₆ N ₂ O ₂	C ₁₈ H ₁₈ N ₂ O ₂	C ₁₅ H ₂₂ N ₂ O ₈
Fw	208.69	286.81	232.28	294.35	358.35
Temperature/K	293(2)	293(2)	293(2)	293(2)	293(2)
Crystal system	Triclinic	Monoclinic	Orthorhombic	Monoclinic	Orthorhombic
Space group	<i>P</i> $\bar{1}$	<i>P</i> 2 ₁ / <i>n</i>	<i>Pbca</i>	<i>P</i> 2 ₁ / <i>c</i>	<i>P</i> 2 ₁ ·2 ₁
<i>a</i> /Å	7.0715(14)	6.9883(14)	17.755(4)	24.339(5)	7.1192(14)
<i>b</i> /Å	9.0663(18)	17.034(3)	7.4749(15)	7.2309(14)	15.328(3)
<i>c</i> /Å	17.098(3)	12.698(3)	18.786(4)	18.639(4)	15.729(3)
α (°)	92.53(3)	90.00	90.00	90.00	90
β (°)	101.12(3)	99.88(3)	90.00	112.50(3)	90
γ (°)	102.62(3)	90.00	90.00	90.00	90
Volume/Å ³	1045.3(4)	1489.1(5)	2493.2(9)	3030.4(10)	1716.4(6)
Z	4	4	8	8	4
<i>D</i> _x /Mg m ⁻³	1.326	1.279	1.238	1.290	1.387
<i>F</i> (000)	440	608	992	1248	760
θ range for data collection	3.01° to 27.48°	2.02° to 27.48°	3.15° to 27.46°	23.06° to 27.48°	3.14° to 27.48°
Limiting indices	-9 ≤ <i>h</i> ≤ 9, -11 ≤ <i>k</i> ≤ 11, -20 ≤ <i>l</i> ≤ 22	0 ≤ <i>h</i> ≤ 9, 0 ≤ <i>k</i> ≤ 22, -16 ≤ <i>l</i> ≤ 16	-23 ≤ <i>h</i> ≤ 22, -9 ≤ <i>k</i> ≤ 9, -24 ≤ <i>l</i> ≤ 24	-31 ≤ <i>h</i> ≤ 31, -9 ≤ <i>k</i> ≤ 8, -24 ≤ <i>l</i> ≤ 23	-9 ≤ <i>h</i> ≤ 8, -19 ≤ <i>k</i> ≤ 19, -20 ≤ <i>l</i> ≤ 19
Data/restraints/parameters	4741/0/281	3411/0/218	2480/0/169	6913/0/426	2250/0/254
Goodness-of-fit on <i>F</i> ²	1.081	0.937	1.044	1.036	1.045
Final <i>R</i> indices [<i>I</i> > 2σ(<i>I</i>)]	<i>R</i> ₁ ^a = 0.0435, <i>wR</i> ₂ ^b = 0.1332	<i>R</i> ₁ ^a = 0.0452, <i>wR</i> ₂ ^b = 0.1211	<i>R</i> ₁ ^a = 0.0522, <i>wR</i> ₂ ^b = 0.1345	<i>R</i> ₁ ^a = 0.0592, <i>wR</i> ₂ ^b = 0.1247	<i>R</i> ₁ ^a = 0.0483, <i>wR</i> ₂ ^b = 0.1351
<i>R</i> indices (all data)	<i>R</i> ₁ ^a = 0.0593, <i>wR</i> ₂ ^b = 0.1501	<i>R</i> ₁ ^a = 0.0757, <i>wR</i> ₂ ^b = 0.1349	<i>R</i> ₁ ^a = 0.0873, <i>wR</i> ₂ ^b = 0.1495	<i>R</i> ₁ ^a = 0.1150, <i>wR</i> ₂ ^b = 0.1442	<i>R</i> ₁ ^a = 0.0550, <i>wR</i> ₂ ^b = 0.1391
Largest diff. peak and hole/e.Å ⁻³	0.380 and -0.309	0.338 and -0.280	0.211 and -0.156	0.211 and -0.165	0.253 and -0.192
^a <i>R</i> ₁ = $\sum F_o - F_c / \sum F_o $, ^b <i>wR</i> ₂ = $\sqrt{\sum [w(F_o^2 - F_c^2)]^2} / \sum [w(F_o^2)]}$					

Table 2 Hydrogen-Bond Geometries for 1·HCl, 1·HCl-DMSO, 1·HCOOH and 1·CH₃COOH

Structure	D–H···A	<i>d</i> (D–H) (Å)	<i>d</i> (H···A) (Å)	<i>d</i> (D···A) (Å)	<(DHA) (°)
1·HCl ^a	C(7)–H(7)···Cl(1)#1	0.93	2.77	3.627(2)	154.4
	C(10)–H(10C)···Cl(1)#2	0.96	3.00	3.943(3)	168.9
	C(18)–H(18)···Cl(1)#3	0.93	2.79	3.581(2)	143.7
	C(21)–H(21C)···Cl(1)	0.96	2.78	3.691(3)	159.7
	C(22)–H(22C)···Cl(2)#4	0.96	2.90	3.857(2)	175.6
	N(1)–H(100)···Cl(1)#5	0.96(2)	2.13(3)	3.0916(17)	176(2)
	N(2)–H(101)···Cl(2)#5	0.90(3)	2.52(3)	3.402(3)	166(2)
	N(2)–H(102)···Cl(1)#1	0.81(3)	2.85(3)	3.648(2)	166(3)
	N(3)–H(103)···Cl(2)#6	0.89(3)	2.25(3)	3.142(2)	176(2)
	N(4)–H(104)···Cl(1)#3	0.97(2)	2.43(3)	3.373(2)	162(2)
	N(4)–H(105)···Cl(2)#3	0.90(3)	2.70(3)	3.514(2)	151.5(19)
	N(1)–H(1)···Cl(1)#1	0.91(3)	2.19(3)	3.1007(19)	179(3)
	N(2)–H(2A)···O(1)#1	0.91(3)	1.92(3)	2.832(3)	176(3)
	N(2)–H(2B)···Cl(1)	0.76(3)	2.51(3)	3.267(3)	174(2)
1·HCl-DMSO ^b	C(8)–H(8)···Cl(1)	0.92(2)	3.01(2)	3.773(2)	140.4(17)
	C(12)–H(12C)···O(1)#2	0.96	2.62	3.463(4)	146.5
	C(13)–H(13C)···O(1)#3	0.96	2.87	3.692(4)	144.6
	N(1)–H(1)···O(2)#1	0.99(3)	1.69(3)	2.660(2)	167(2)
	N(2)–H(2B)···O(1)#2	0.86	2.13	2.954(3)	159.8
	N(2)–H(2A)···O(1)#3	0.86	2.08	2.908(2)	162.6
	C(8)–H(8)···O(2)#2	0.93	2.56	3.484(3)	169.8
	C(11)–H(11A)···O(2)#1	0.96	2.64	3.343(3)	130.8
	C(11)–H(11C)···O(2)#4	0.96	2.64	3.593(3)	173.1
	C(11)–H(11B)···O(1)#5	0.96	2.78	3.622(3)	146.9
	N(2)–H(101)···O(2)#1	0.93(3)	2.14(3)	2.992(2)	152(2)
	N(2)–H(100)···O(1)#2	0.87(3)	2.06(3)	2.930(2)	172(2)
	N(1)–H(1)···O(1)#3	1.04(2)	2.58(2)	3.236(2)	120.7(15)
	N(1)–H(1)···O(2)#3	1.04(2)	1.57(2)	2.607(2)	173(2)
1·HCOOH ^c	C(2)–H(2)···O(1)#4	0.93	2.74	3.507(2)	140.4
	C(8)–H(8)···O(2)#3	0.93	2.69	3.334(2)	127.4
	C(10)–H(10C)···O(1)#3	0.96	2.61	3.295(3)	128.5
	C(10)–H(10B)···O(1)#4	0.96	2.63	3.527(3)	155.5

^a #1 *x*, *y* + 1, *z* + 1; #2 $-x$, $-y$, $-z$ + 1; #3 $-x$ + 1, $-y$, $-z$ + 1; #4 $-x$ + 1, $-y$ + 1, $-z$ + 1; #5 *x*, *y*, *z* + 1; #6 *x*, *y* – 1, *z*. ^b #1 $-x$ + 1/2, *y* + 1/2, $-z$ + 1/2; #2 $-x$ + 1, $-y$, $-z$ + 1; #3 $-x$, $-y$, $-z$ + 1. ^c #1 *x*, *y*, *z* – 1; #2 *x*, *y* + 1, *z* – 1; #3 $-x$, $-y$ + 2, $-z$; #4 $-x$ + 1, $-y$ + 1, $-z$ + 1; #5 $-x$, $-y$ + 1, $-z$ + 1. ^d #1 $-x$ + 1, $-y$, $-z$ + 1; #2 *x* – 1, $-y$ + 1/2, *z* + 1/2; #3 *x* – 1, *y*, *z*.

Table 3 Hydrogen-Bond Geometries for 1·PhCOOH and 1·L-tartaric acid, together with C–H···π interaction parameters for 1·PhCOOH

Structure	D–H···A	<i>d</i> (D–H) (Å)	<i>d</i> (H···A) (Å)	<i>d</i> (D···A) (Å)	<(DHA) (°)
1·PhCOOH ^a	N(1)–H(100)···O(2)#1	1.11(3)	1.56(3)	2.628(2)	161(2)
	N(3)–H(101)···O(4)	0.94(2)	1.74(2)	2.657(2)	165(2)
	N(2)–H(103)···O(1)#2	0.92(3)	2.01(3)	2.927(3)	177(3)
	N(4)–H(105)···O(3)#3	0.86(3)	2.09(3)	2.940(3)	169(3)
	C(2)–H(2)···Cg(1)	0.929	2.828	3.7452(31)	169.342(181)
	C(13)–H(13)···Cg(2)#4	0.929	2.829	3.7464(26)	169.660(157)
	N(4)–H(105)···Cg(1)#5	0.86(4)	3.24(3)	3.97(4)	146.171(251)
	O(8)–H(106)···O(4)	0.93	2.56	2.788(3)	94.0
	O(7)–H(104)···O(8)#1	0.97(3)	1.84(3)	2.743(4)	153(3)
	O(7)–H(103)···O(1)#2	0.86(6)	2.00(6)	2.832(3)	165(5)
1·L-tartaric acid ^b	N(1)–H(102)···O(3)#3	0.76(4)	2.31(4)	2.930(3)	140(3)
	N(1)–H(102)···O(1)#3	0.76(4)	2.22(4)	2.886(3)	148(4)
	N(2)–H(101)···O(7)#4	1.15(3)	1.98(3)	2.943(6)	139(2)
	N(2)–H(100)···O(5)#4	0.95(7)	2.31(7)	3.006(4)	130(6)
	O(4)–H(4)···O(6)	0.82	2.07	2.576(3)	119.4
	O(3)–H(3)···O(7)	0.82	1.94	2.756(3)	176.7
	C(2)–H(2)···O(2)#5	0.93	2.62	3.533(4)	165.5
	C(10)–H(10C)···O(8)#2	0.96	2.60	3.499(5)	156.3
	C(10)–H(10B)···O(4)	0.96	2.71	3.405(4)	129.5
	C(10)–H(10B)···O(6)	0.96	2.86	3.303(4)	109.4
	C(13)–H(13)···N(2)#6	0.98	2.60	3.526(4)	156.9
	O(2)–H(107)···O(5)#7	0.94(6)	1.55(6)	2.457(2)	161(5)
	O(2)–H(107)···O(6)#7	0.94(6)	2.63(5)	3.307(3)	130(4)
	C(7)–H(7)···O(8)#8	0.93	2.81	3.714(5)	165.8
	C(11)–H(11C)···O(6)#9	0.96	2.91	3.338(6)	108.2

^a #1 $-x$ + 1, *y* + 1/2, $-z$ + 1/2; #2 $-x$ + 1, $-y$, $-z$ + 1; #3 *x*, $-y$ + 3/2, *z* + 1/2; #4 *x* – 1, *y*, *z*; #5 $-x$ + 1, $-y$ + 1, $-z$ + 1; Cg1 and Cg2 are the centroids of the phenyl rings C23/C24/C25/C26/C27/C28 and C30/C31/C32/C33/C34/C35, respectively. ^b #1 $-x$ + 1, *y* – 1/2, $-z$ + 1/2; #2 *x* – 1, *y*, *z*; #3 $-x$ + 1, *y* + 1/2, $-z$ + 1/2; #4 *x*, *y* + 1, *z*; #5 *x* – 1/2, $-y$ + 1/2, $-z$; #6 *x*, *y* – 1, *z*; #7 *x* + 1, *y*, *z*; #8 *x* – 1/2, $-y$ + 3/2, $-z$; #9 $-x$ + 1/2, $-y$ + 1, *z* – 1/2.

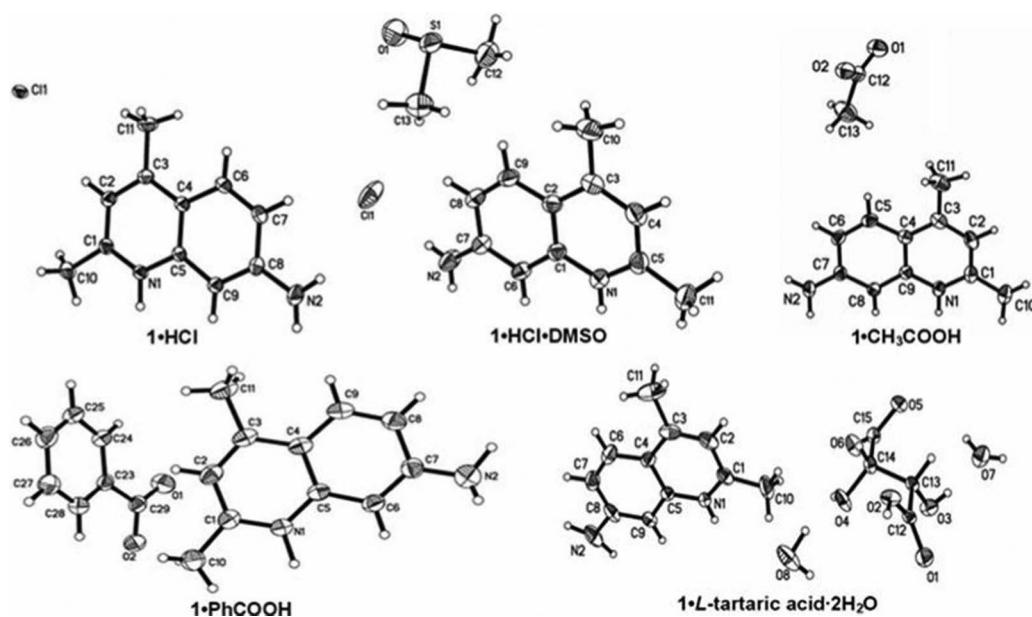


Fig. 1 Molecular structures of 1·HCl, 1·HCl·DMSO, 1·CH₃COOH, 1·PhCOOH, 1·L-tartaric acid·2H₂O; The thermal ellipsoids are drawn at 30% probability levels.

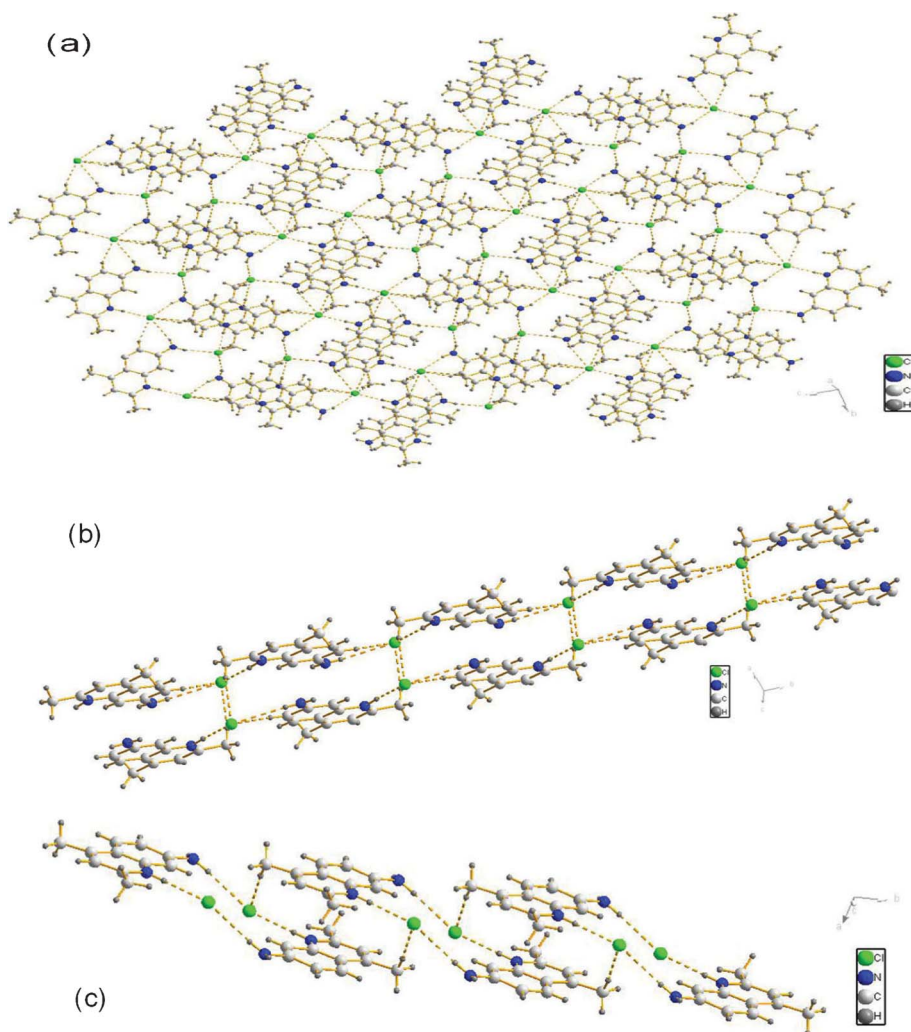


Fig. 2 (a) Perspective view of crystal packing of 1·HCl; (b) the 2D layer structure formed by molecule A; (c) the ladder structure formed by molecule B. The asymmetric unit contains two independent molecules A and B; the hydrogen bonds are indicated in yellow dashed lines.

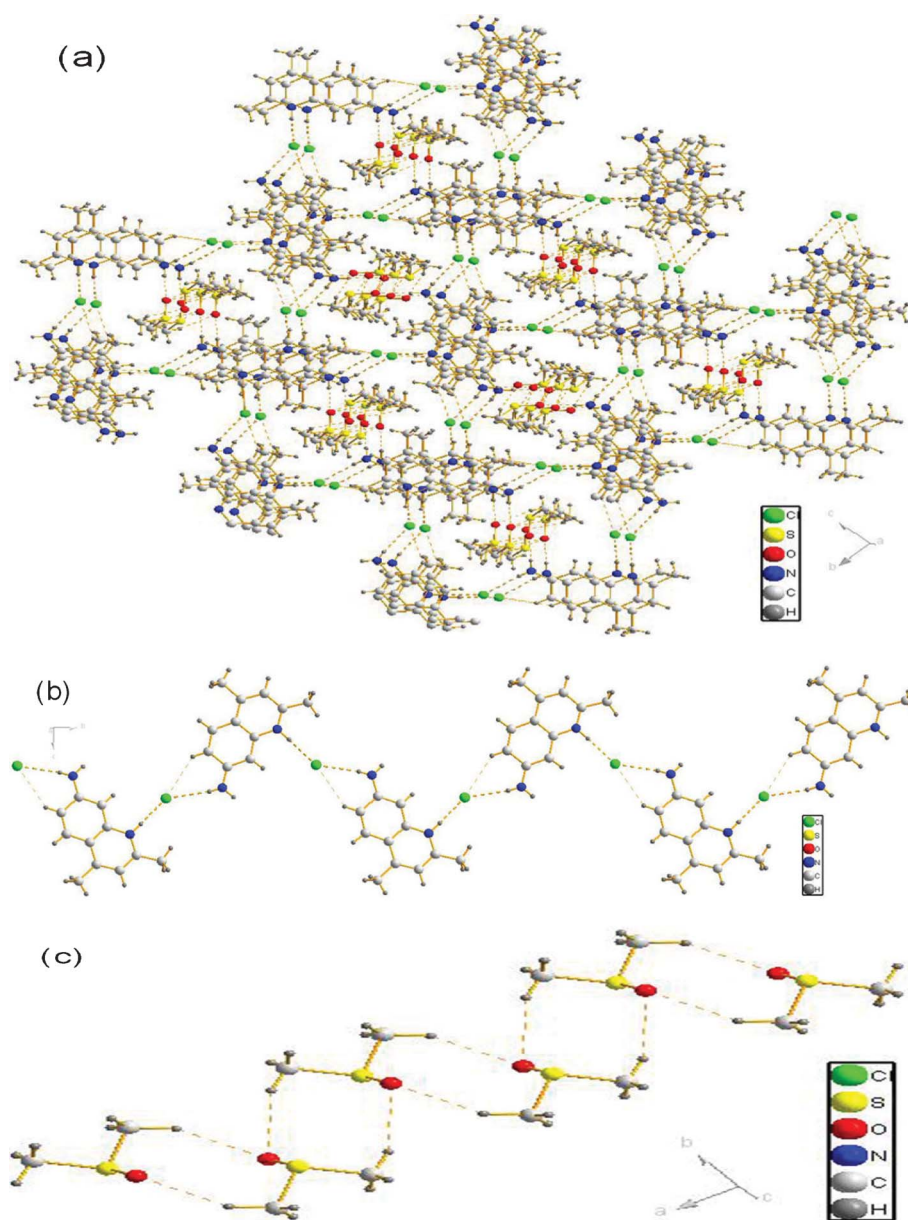


Fig. 3 (a) Perspective view of crystal packing of **1-HCl-DMSO**; (b) 1-D S-shape chain formed by N-H \cdots Cl and C-H \cdots Cl interactions; (c) the infinite 1-D chain formed by DMSO molecules. The hydrogen bonds are indicated in yellow dashed lines.

separation distance of 3.24 and 3.68 Å. The quinoline rings are almost parallel with the dihedral angle of 2.8°.

7-Amino-2,4-dimethylquinolinium benzoate crystallizes in the monoclinic space group $P2_1/c$. The asymmetric unit contains two independent molecules A and B, shown in Fig. 1 (molecular A), and Fig. S1, ESI, \dagger (molecular B). The dihedral angles between the quinolinium ring and the corresponding phenyl ring of the benzoate anion are 109.8° (molecule A) and 84.6° (molecule B), respectively. In molecule A, there are C-H \cdots π interactions between the C-H bond of quinolinium ring and the centroid of the phenyl ring. Meanwhile, in molecule B, there are N3-H101 \cdots O4 hydrogen bonds. In the packing of **1-PhCOOH** (Fig. 6), two adjacent 7-amino-2,4-dimethylquinolinium benzoate in molecule A form a dimer through C-H \cdots π interactions and N-H \cdots O hydrogen bonds (Fig. 6b), while 7-amino-2,4-

dimethylquinolinium benzoate in molecule B form an infinite 1-D chain through N-H \cdots O hydrogen bonds. For molecular A, the dimer units assemble to 3-D network through other N-H \cdots O hydrogen bonds. In the case of molecular B, the adjacent 1-D chains further assemble into 3-D network through C-H \cdots π interactions (Fig. 6c). There also exist π - π interactions between two quinoline rings with the separation distance of 3.42 Å (molecule A) and 3.39 Å (molecule B), respectively. There exist very weak N-H \cdots π interactions between the two 3-D networks formed by molecules A and B, resulting in more complex supramolecular networks.

7-Amino-2,4-dimethylquinolinium tartarate dihydrate crystallizes in the orthorhombic space group $P2_12_12_1$, with one L-tartarate anion, one 7-amino-2,4-dimethylquinolinium and two water molecules in a crystallographically asymmetric unit. More

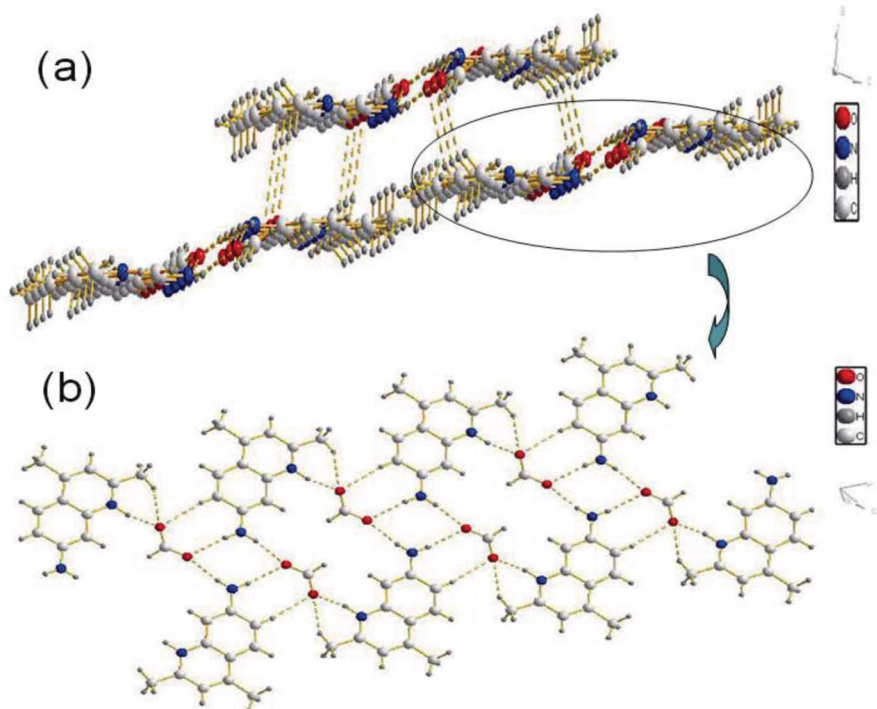


Fig. 4 Perspective view of crystal packing of **1·HCOOH**. (a) The 3-D network formed by 2-D sheets through intermolecular C11–H11C···O2, C11–H11B···O1 and π – π interactions; (b) the 2-D sheet with intermolecular C–H···O interactions and intermolecular N–H···O hydrogen bonds. The hydrogen bonds are indicated in yellow dashed lines.

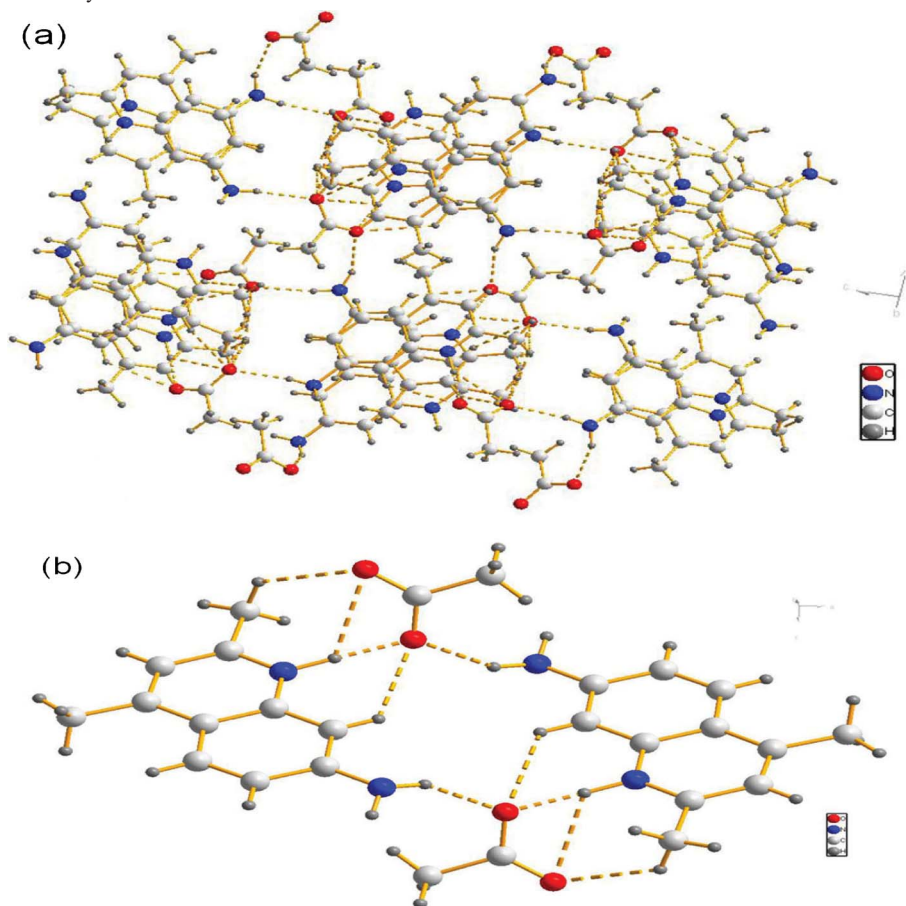


Fig. 5 Perspective view of crystal packing of **1·CH₃COOH**. (a) The 3-D network formed by dimmers through intermolecular C–H···O interactions, intermolecular N–H···O hydrogen bonds and π – π interactions; (b) the dimer with intermolecular C–H···O interactions and intermolecular N–H···O hydrogen bonds. The hydrogen bonds are indicated in yellow dashed lines.

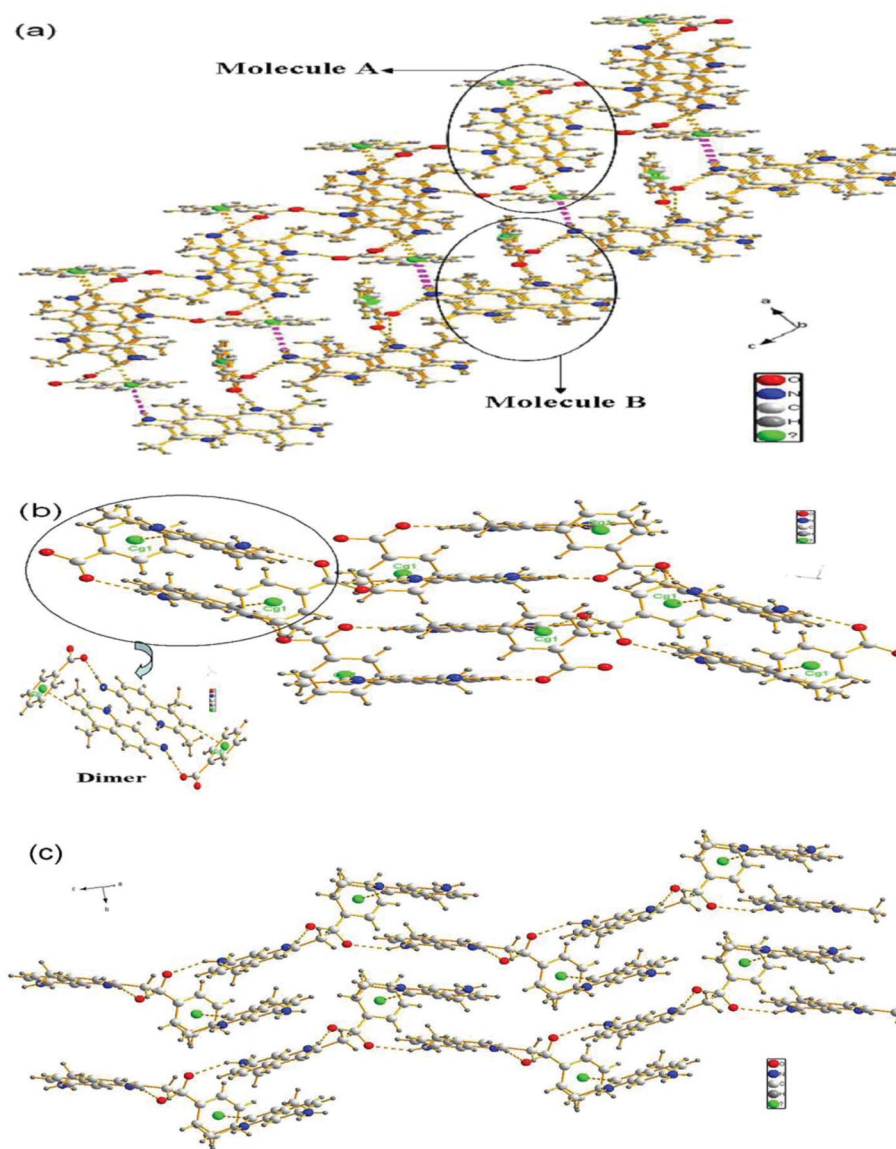


Fig. 6 Perspective view of crystal packing of **1-PhCOOH**. (a) The complex 3-D structure formed by molecule A and molecule B; (b) the 3-D network formed by molecule A through intermolecular C-H...Cg1 interactions, intermolecular N-H...O hydrogen bonds and π - π interactions; (c) the 3-D network formed by molecule B through intermolecular N-H...O hydrogen bonds, C-H...Cg2 interactions and π - π interactions. The asymmetric unit contains two independent molecules A and B. The hydrogen bonds and C-H... π interactions are indicated in yellow dashed lines. The weak N-H... π interactions are indicated in purple dashed lines. Cg1 and Cg2 are the centroids of the phenyl rings C23/C24/C25/C26/C27/C28 and C30/C31/C32/C33/C34/C35, respectively and indicated in green ball.

recently, the intermolecular interactions of (L)-tartaric acid with heteroaromatic amines have been observed in construction of supramolecular architectures¹⁶ and in the use of non-linear optical materials,¹⁷ where the crystal structures of a number of 1 : 1 salts have been determined, allowing a full comparison with 7-amino-2,4-dimethylquinolinium salt. The L-tartarate anion forms a self-association of S(5) motif through an intramolecular O4-H4...O6 hydrogen bond. The intermolecular O2-H107...O5 and O2-H107...O6 hydrogen bonds link the L-tartarate anions in a head-to-tail fashion to an infinite chain along a-axis. The adjacent chains were linked together with two water molecules through O-H...O hydrogen bonds to form 3-D honeycomb network (Fig. 7). A different three-dimensional hydrogen-bonded honeycomb framework through carboxylate interactions

with other tartarate hydroxyl groups, as well as with the water molecules has been described in the tartarate analogue.¹⁶ There exist π - π interactions between the adjacent quinoline rings with the centroid-centroid distance of 3.53 and 3.59 Å, stacking into a column structure along *a* axis direction. The quinoline rings are almost antiparallel to each other, with the dihedral angle of 2.2°. The 3-D network and the column substructure of π -stacked quinolinium cations were further linked together through N-H...O, C-H...O and C-H...N hydrogen bonds.

A comparison of the structures of quinolinium salts indicates that the interesting supramolecular networks were dominated by the strong hydrogen bonding N-H...O/Cl and much weaker C-H...N/Cl, C-H... π and π - π assembling interactions, each playing an important role in controlling their crystal packing.

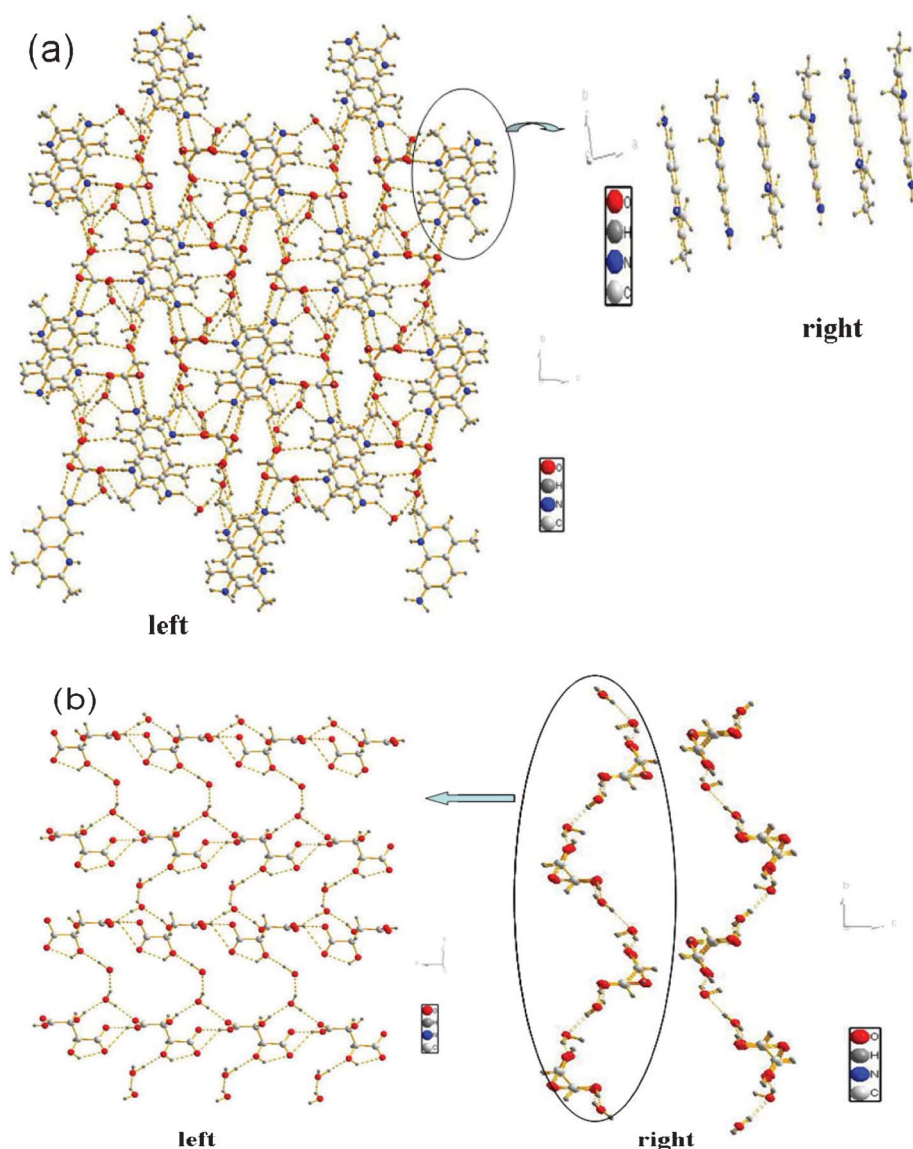


Fig. 7 Perspective view of crystal packing of **1-L-tartaric acid·2H₂O**. (a) the 3-D structure formed by quinolinium, L-tartarate and water molecules through N–H···O, C–H···O, C–H···N, O–H···O hydrogen bonds and π – π interactions (left: the 3-D structure; right: the column structure formed by quinolinium through π – π interactions). (b) the 3-D network formed by L-tartarate and water molecules through O–H···O hydrogen bonds (left: the 3-D network; right: the infinite chain formed by the L-tartarate through the intermolecular O–H···O hydrogen bonds). The hydrogen bonds are indicated in yellow dashed lines.

Notably, the different packing structures are a result of the effect of the anions. In **1·HCl**, the Cl1 atom forms seven hydrogen bonds to four C atoms and three N atoms, but Cl2 atom forms four hydrogen bonds to a C atom and three N atoms. In **1·HCl·DMSO**, the Cl atom forms three hydrogen bonds to two N atoms and a C atom. For both chloride salts, the weak C–H···Cl interactions together with two N–H···Cl hydrogen bonds form rings of a graph-set motif $R_2^1(6)$. In the HCOO[−] and CH₃COO[−] salts, each HCOO[−] and CH₃COO[−] anions are located among three quinolinium cations and form five hydrogen bonds, including three N–H···O and two C–H···O contacts with the graph-set motifs $R_2^1(6)$, $R_2^2(8)$, and $R_4^4(20)$ for **1·HCOOH** and motifs $R_2^1(6)$ and $R_4^2(12)$ for **1·CH₃COOH**. In the PhCOO[−] salt, each PhCOO[−] anion is located among three quinolinium cations and form two hydrogen bonds being N–H···O and a C–H··· π

interaction. In the L-HOOCCH(OH)CH(OH)COO[−] salt, each L-HOOCCH(OH)CH(OH)COO[−] anion is located among three quinolinium cations and form five hydrogen bonds, including two N–H···O, two C–H···O and a C–H···N contacts with the graph-set motifs $R_2^1(6)$ and $R_2^2(7)$. Specifically, **1·HCl** and **1·HCl·DMSO** exhibit 1-D chain based on the interlinked quinolinium molecules by N–H···Cl hydrogen bonds. In the packing arrangement, the adjacent chain was held together by π – π interactions between adjacent quinoline rings to form the layer structure. In **1·HCl**, the adjacent dimers with ring motif $R_4^2(16)$ are further held together by C–H···Cl and π – π interactions, leading to formation of a ladder structure. Thus, the layer structure and ladder structure were interlinked through N–H···Cl, C–H···Cl interactions to form the extending 3-D network structure. In the case of **1·HCl·DMSO**, the layer structure together with the 1-D S-shape chain formed by DMSO molecules were further linked through

N–H···O hydrogen bonds to form the final 3-D network. In the packing of **1·HCOOH**, the adjacent sheets were linked together through C–H···O and π – π interactions to form 3-D network. In **1·CH₃COOH**, the dimmers were linked together through N–H···O, C–H···O and π – π interactions to form 3-D network. In the PhCOO[−] salt, the adjacent chains were held together by C–H··· π interactions to assemble into 3-D network, and the dimmer units were linked together through N–H···O hydrogen bonds to form another 3-D network. Furthermore, the two 3-D networks are linked together by weak N–H··· π interactions to form more complex supramolecular networks. In the L-HOOCCH(OH)CH(OH)COO[−] salt, the infinite chains were formed by O–H···O hydrogen bonds between adjacent L-tartrate anions in a head-to-tail fashion, which further linked together with two water molecules through O–H···O hydrogen bonds to form 3-D honeycomb network. The 3-D network and the column substructure of π -stacked quinolinium cations were further interlinked together through N–H···O, C–H···O and C–H···N hydrogen bonds, resulting in a novel 3-D network.

Luminescent properties of compounds **1**, **1·HCl**, **1·HCOOH**, **1·CH₃COOH**, **1·PhCOOH** and **1·L-tartaric acid**

The photophysical properties of the quinoline compound **1** and the corresponding salts **1·HCl**, **1·HCOOH**, **1·CH₃COOH**, **1·PhCOOH**, and **1·L-tartaric acid** were investigated by UV/vis and photoluminescence (PL) spectroscopy in solutions and in the solid state at room temperature. The obtained spectral data are summarized in Supporting Information Table ST-1, ESI.†

The emission spectra of the quinolinium compounds in the solid state are shown in Fig. 8, with strongly broadened asymmetric emission bands compared to the observed emission for the compound **1**. All compounds produce bright fluorescence in the solid state with emission maxima of 422, 534, 506, 484, 519 and 524 nm, respectively, with the red shift of about 62–112 nm compared with the emission maximum of compound **1**. The fluorescent emissions of the quinolinium compounds can mainly be assigned to the π – π^* transitions of the aminoquinolinium moieties and the charge-transfer (CT) transitions between anions

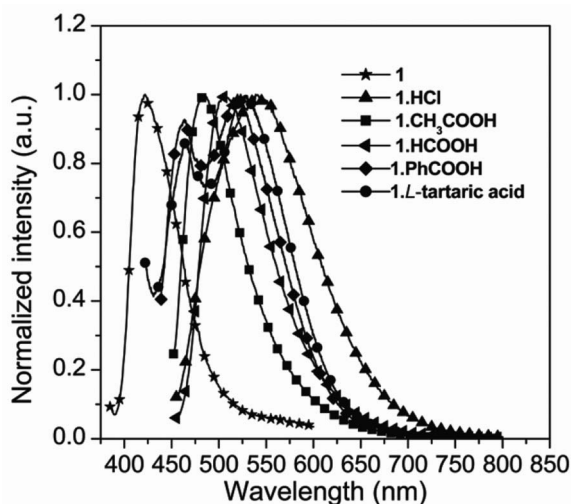


Fig. 8 Emission spectra of **1**, **1·HCl**, **1·HCOOH**, **1·CH₃COOH**, **1·PhCOOH** and **1·L-tartaric acid** in the solid state.

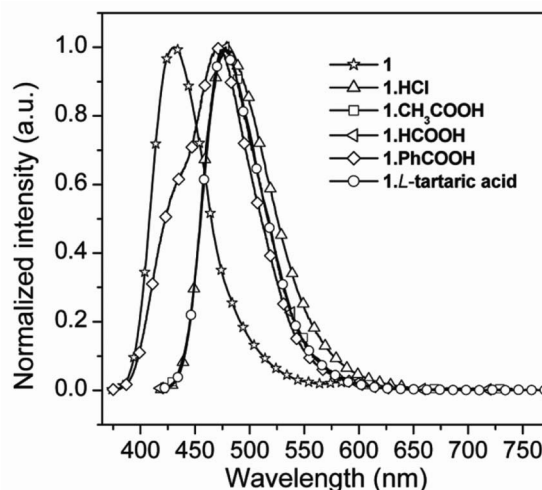


Fig. 9 Emission spectra of **1**, **1·HCl**, **1·HCOOH**, **1·CH₃COOH**, **1·PhCOOH** and **1·L-tartaric acid** in EtOH solution.

and the quinolinium cations, in accordance with the other related studies in the literature.¹⁸ A significant red shift of the emission bands had been investigated in the phenanthroline salts in comparison with those of 1,10-phenanthroline.¹⁹ Moreover, it was revealed by the density functional theory (DFT) calculations that the red shift emission is attributed to a decreased energy gap between the highest occupied molecular orbital (HOMO) and lowest unoccupied molecular orbital (LUMO) involved in the CT transition.²⁰ Interestingly, the solid-state emission spectra of the quinolinium compounds are sensitive to the noncovalent interactions.²¹ The hydrogen bonding N–H/O/Cl are involved in interaction of quinolinium cation with anions, and further affect energy levels of the excited states. It has also been reported that the intermolecular hydrogen bonding can significantly tune the energy levels and further influence the spectral properties of hydrogen bond-mediated complexes.²² In this respect, the hydrogen bond-mediated complexation of tartaric acid with quinoline based receptors results in monomer emission quenching followed by intramolecular excimer emission.²³ In addition, crystal structure analysis of quinolinium compounds showed that the quinolinium moieties are involved in π – π stacking and C–H– π interactions and they are also expected to induce the red-shifted emission.^{20b,24}

The typical emission spectra of the quinolinium compounds in EtOH are also shown in Fig. 9. The solution photoluminescence spectral maxima of the quinolinium salts are blue-shifted compared with their solid-state emission spectra, similar to that seen in previous observations.²⁵ The red shift of the emission maxima from solution to solid state is due to π – π stacking interactions between the quinolinium aromatic rings in solid state.

Conclusions

A number of 7-amino-2,4-dimethylquinolinium salts with different anions have been synthesized and characterized. The structure analysis confirms that the nitrogen atoms in the quinoline rings are protonated in all salts. The two solvates have been obtained and thereby provide a useful complement to

cocrystal screening. All the quinolinium salts display interesting three dimension supramolecular networks. The strong hydrogen bonding N/O–H···O and N–H···Cl, together with weak C–H···O/N/Cl hydrogen bonds become prominent in the construction of the observed supramolecular networks. Their crystal packing is also stabilized by C/N–H··· π contacts and π – π stacking interactions. The 7-amino-2,4-dimethylquinolinium salts show strong luminescence in the solid state and organic solution in the range 422–534 nm. The emission wavelength of the salts can be tuned by changing the anion species. The solid-state emission spectra of the quinolinium salts are highly dependent on the nature of the stacking interactions. The results also demonstrated that a family of quinolinium salts should be considered as the promising candidates for potential solid-state photofunctional materials.

Acknowledgements

This work was supported by the National Natural Science Foundation of China (Nos. 21004026 and 21074043). We are also grateful for support by the Frontiers of Science and Interdisciplinary Innovation Project of Jilin University (Nos. 450060445023 and 450060445027).

References

- (a) M. C. Etter, *Acc. Chem. Res.*, 1990, **23**, 120; (b) P. Metrangolo, H. Neukirch, T. Pilati and G. Resnatti, *Acc. Chem. Res.*, 2005, **38**, 386; (c) D. A. Britz and A. N. Khlobystov, *Chem. Soc. Rev.*, 2006, **35**, 637; (d) B. Moulton and M. J. Zaworotko, *Chem. Rev.*, 2001, **101**, 1629.
- (a) T. Steiner, *Angew. Chem., Int. Ed.*, 2002, **41**, 48; (b) K. Kinbara, Y. Hashimoto, M. Sukeyawa, H. Nohira and K. Saigo, *J. Am. Chem. Soc.*, 1996, **118**, 3441; (c) D. V. Soldatov, I. L. Moudrakovski, E. V. Grachev and J. A. Ripmeester, *J. Am. Chem. Soc.*, 2006, **128**, 6737; (d) C. C. Seaton, A. Parkin, C. C. Wilson and N. Bladen, *Cryst. Growth Des.*, 2009, **9**, 47; (e) C. G. Bazuin and F. A. Brandys, *Chem. Mater.*, 1992, **4**, 970.
- (a) G. R. Desiraju and T. Steiner, *The Weak Hydrogen Bond in Structural Chemistry and Biology*, Oxford University Press, Oxford, 2001; (b) J. L. Atwood and J. W. Steed, *Encyclopedia of Supramolecular Chemistry*, Marcel Dekker, New York, 2004 (c) J. W. Steed and J. L. Atwood, *Supramolecular Chemistry*, 2nd edition, Wiley, Chichester, 2009.
- (a) C. H. Görbitz, M. Nilsen, K. Szeto and L. W. Tangen, *Chem. Commun.*, 2005, 4288; (b) M. Du, Z.-H. Zhang, W. Guo and X.-J. Fu, *Cryst. Growth Des.*, 2009, **9**, 1655; (c) K. Kodama, Y. Kobayashi and K. Saigo, *Cryst. Growth Des.*, 2007, **7**, 935; (d) D. Braga, L. Brammer and N. R. Champness, *CrystEngComm*, 2005, **7**, 1; (e) K. Biradha, *CrystEngComm*, 2003, **5**, 374.
- P. Barthélémy, S. J. Lee and M. Grinstaff, *Pure Appl. Chem.*, 2005, **77**, 2133.
- (a) J. Pitha, M. Akashi, M. Draminski and In, *Biomedical Polymers*, E. P. Goldberg and A. Nakajima (ed.), p. 271, Academic Press, New York, 1980; (b) D. F. Doyle, D. A. Braasch, C. G. Simmons, B. A. Janowski and D. A. Corey, *Biochemistry*, 2001, **40**, 53; (c) H. Kuhn, V. V. Demidov, J. M. Coull, M. J. Fiandaca, B. D. Gildea and M. D. Frank-Kamenetskii, *J. Am. Chem. Soc.*, 2002, **124**, 1097; (d) A. Okamoto, K. Tanabe and I. Saito, *J. Am. Chem. Soc.*, 2002, **124**, 10262.
- (a) N. Schultheiss, K. Lorimer, S. Wolfe and J. Desper, *CrystEngComm*, 2010, **12**, 742; (b) K. Chow, H. H. Y. Tong, S. Lum and A. H. L. Chow, *J. Pharm. Sci.*, 2008, **97**, 2855; (c) S. L. Childs and M. J. Zaworotko, *Cryst. Growth Des.*, 2009, **9**, 4208; (d) T. Rager and R. Hilfiker, *Cryst. Growth Des.*, 2010, **10**, 3237; (e) S.-L. Zheng, J.-M. Chen, W.-X. Zhang and T.-B. Lu, *Cryst. Growth Des.*, 2011, **11**, 466.
- (a) T. R. Shatock, K. K. Arora, P. Visheshwar and M. J. Zaworotko, *Cryst. Growth Des.*, 2008, **8**, 4533; (b) S. Mohamed, D. A. Tocher, M. Vickers, P. G. Karamertzanis and S. L. Price, *Cryst. Growth Des.*, 2009, **9**, 2881; (c) D. Singh, P. K. Bhattacharyya and J. B. Baruah, *Cryst. Growth Des.*, 2010, **10**, 348; (d) C. B. Aakeröy, M. E. Fasulo and J. Desper, *Mol. Pharmaceutics*, 2007, **4**, 317.
- (a) P. Visheshwar, A. Naryia and V. M. Lynch, *J. Org. Chem.*, 2002, **67**, 556; (b) S. Aitipamula, P. K. Thallapally, R. Thaimattam, M. Jaskolski and G. R. Desiraju, *Org. Lett.*, 2002, **4**, 921; (c) G. R. Desiraju and T. Steiner, *The Weak Hydrogen Bond in Structural Chemistry and Biology*, Oxford University Press: Oxford, 1999.
- (a) V. Berl, I. Huc, R. G. Khoury, M. J. Krische and J. M. Lehn, *Nature*, 2000, **407**, 720; (b) N. Stanley, V. Sethuraman, P. T. Muthiah, P. Luger and M. Weber, *Cryst. Growth Des.*, 2002, **2**, 631; (c) S. Baskar Raj, P. T. Muthiah, U. Rychlewskab and B. Warzajtisb, *CrystEngComm*, 2003, **5**, 48; (d) V. Berl, M. J. Krische, I. Huc, J.-M. Lehn and M. Schmitz, *Chem.-Eur. J.*, 2000, **6**, 1938.
- (a) Q. Su, W. Gao, Q.-L. Wu, L. Ye, G.-H. Li and Y. Mu, *Eur. J. Inorg. Chem.*, 2007, 4168; (b) Q. Su, Q.-L. Wu, G.-H. Li, X.-M. Liu and Y. Mu, *Polyhedron*, 2007, **26**, 5053.
- Q. Su, L. Ye, G.-D. Yang and Y. Mu, *Acta Crystallogr., Sect. E: Struct. Rep. Online*, 2007, **63**, o1699.
- G. M. Sheldrick, *SHELXTL*; PC Siemens Analytical X-ray Instruments: Madison WI, 1993.
- (a) G. M. Sheldrick, *Acta Crystallogr., Sect. A: Found. Crystallogr.*, 2008, **64**, 112; (b) G. M. Sheldrick, *SHELXTL Structure Determination Programs*, Version 5.0; PC Siemens Analytical Systems: Madison, WI, 1994.
- E. Roberts and E. Turner, *J. Chem. Soc.*, 1927, 1832.
- G. Smith, U. D. Wermuth and J. M. White, *Acta Crystallogr., Sect. C: Cryst. Struct. Commun.*, 2006, **62**, o694.
- (a) J. Fuller, R. T. Carlin, L. J. Simpson and T. E. Furtak, *Chem. Mater.*, 1995, **7**, 909; (b) M. K. Marchewska, S. Debrus, A. Pietraszko, A. J. Barnes and H. Ratajczak, *J. Mol. Struct.*, 2003, **656**, 265; (c) S. Manivannan, S. Dhanuskodi, K. Kirchbaum and S. K. Tiwari, *Cryst. Growth Des.*, 2006, **6**, 1285; (d) M. K. Marchewska, J. Baran, A. Pietraszko, A. Haznar, S. Debrus and H. Ratajczak, *Solid State Sci.*, 2003, **5**, 509.
- (a) L. M. Scolaro, G. Alibrandi, R. Romeo and V. Ricevuto, *Inorg. Chem.*, 1992, **31**, 2074; (b) K. A. Zachariasse, S. I. Druzhinin, W. Bosch and R. Machinek, *J. Am. Chem. Soc.*, 2004, **126**, 1705 (c) A. N. Swinburne, M. J. Paterson, A. Beeby and J. W. Steed, *Org. Biomol. Chem.*, 2010, **8**, 1010.
- T. Cardinaels, K. Lava, K. Goossens, S. V. Eliseeva and K. Binnemans, *Langmuir*, 2011, **27**, 2036.
- (a) R. Sánchez-de-Armas, J. O. López, M. A. San-Miguel and J. F. Sanz, *J. Chem. Theory Comput.*, 2010, **6**, 2856; (b) S. Patra, R. Gunupuru, R. Lo, E. Suresh, B. Ganguly and P. Paul, *New J. Chem.*, 2012, **36**, 988.
- (a) Q. Wu, Q. Peng, Y. Niu, X. Gao and Z. Shuai, *J. Phys. Chem. A*, 2012, **116**, 3881; (b) Y. Fan, Y. Zhao, L. Ye, B. Li, G. Yang and Y. Wang, *Cryst. Growth Des.*, 2009, **9**, 1421; (c) M. F. Budyka, K. F. Sadykova, T. N. Gavrishova and V.Y. Gak, *High Energy Chem.*, 2000, **46**, 38.
- G.-J. Zhao and K.-L. Han, *Phys. Chem. Chem. Phys.*, 2010, **12**, 8914.
- K. Ghosh and S. Adhikari, *Tetrahedron Lett.*, 2006, **47**, 3577.
- (a) C. P. Price, A. L. Grzesiak and A. J. Matzger, *J. Am. Chem. Soc.*, 2005, **127**, 5512; (b) M. Rafilovich and J. Bernstein, *J. Am. Chem. Soc.*, 2006, **128**, 12185.
- (a) T. Ozdemir, S. Atilgan, I. Kutuk, L. T. Yildirim, A. Tulek, M. Bayindir and E. U. Akkaya, *Org. Lett.*, 2009, **11**, 2105; (b) T.-I. Ho, A. Elangovan, H.-Y. Hsu and S.-W. Yang, *J. Phys. Chem. B*, 2005, **109**, 8626.